

Giant magnetoresistance due to a domain wall in Fe: *Ab initio* study

B. Yu. Yavorsky* and I. Mertig

Martin-Luther Universität Halle-Wittenberg, Fachbereich Physik, D-06099, Halle, Germany

A. Ya. Perlov

Ludwig-Maximilian-Universität München, Fakultät für Chemie und Pharmazie, D-81377 München, Germany

A. N. Yaresko

Max-Planck-Institut für Chemische Physik fester Stoffe, D-01187 Dresden, Germany

V. N. Antonov

Institute for Metal Physics NASU, 03680, Kyiv, Ukraine

(Received 27 June 2002; published 13 November 2002)

The magnetoresistance due to a domain wall in pure Fe was studied theoretically by means of *ab initio* electronic structure calculations based on a linear muffin-tin orbital method modified for noncollinear magnets. The Bloch walls were modeled by a superlattice structure in the (001) direction of the bcc lattice with alternating regions of collinear and spiral-like magnetizations. The conductivity was calculated by means of the linearized Boltzmann equation in a relaxation time approximation. The magnetoresistance due to a domain wall (DW) is presented as a function of the angle between the magnetizations, domain-wall thickness, and domain size. The orientation dependence of the magnetoresistance due to a DW in pure Fe has cos-like behavior in contrary to the giant magnetoresistance in Fe/Cr superlattices. It was also shown that the presence of Cr increases the GMR amplitude in comparison with pure Fe separated by a noncollinear domain wall of equal size. The Kronig-Penney model was used in order to show that the oscillations of GMR as a function of domain size stem from quantum well states crossing the Fermi level.

DOI: 10.1103/PhysRevB.66.174422

PACS number(s): 75.70.Pa, 75.70.Cn, 71.20.Be, 75.60.Ch

I. INTRODUCTION

The discovery of giant magnetoresistance (GMR) in magnetic multilayers¹ renewed the interest in the magnetoresistive properties of domain walls in ferromagnetic systems. The presence of a 180° domain wall (DW) between two regions of opposite magnetization is of particular interest since it reveals GMR. The difference to a standard GMR system is that the interlayer consists of the same material as the regions of collinear magnetic order but is characterized by a noncollinear magnetic order.

The dependence of the resistance of iron on the domain structure was measured experimentally already in the 1950s and 1960s.² But the conditions of these early experiments did not allow a pure contribution due to a DW to be distinguished from other phenomena like galvanomagnetic and size effects. The early theoretical work of Cabrera and Falicov,³ intended to explain these measurements, was based on a free-electron model. The resistivity of a DW was modeled by spin-dependent tunneling through the barrier created by the noncollinear magnetization inside the wall. In this approach the influence of a DW on the electron transport is attributed to the shortening of a mean free path due to reflection from the barrier. For the typical values of the exchange splitting and the DW thickness in ferromagnetic transition metals the increase of the resistivity caused by a DW predicted by this model does not exceed 0.01%

The first indirect, i.e., extracted from the anisotropic magnetoresistance (AMR), experimental observation of the contribution of a DW in a granular epitaxial film of Co and Ni

was reported by Viret *et al.*⁴ The same authors also reported direct measurements of the GMR due to a DW in a single-crystal thin film of Co with a striped domain magnetic structure.⁵ Levy and Zhang⁶ suggested a theoretical treatment of these measurements using the model approach developed previously by these authors for the explanation of the GMR in Fe/Cr multilayers.⁷ The Hamiltonian of the model includes the Kronig-Penney potential for the ferromagnetic regions of opposite magnetization, the potential due to the noncollinear magnetic order in the DW, as well as the spin-dependent scattering potential. For the typical values of the Fermi wave vector, the exchange splitting, and the asymmetry of the different spin channels in Co, Ni, and Fe the additional resistance due to a 150-Å-thick DW varied from 0.3% to 1.8% for the current parallel to the wall and from 2% to 11% for the current perpendicular to the wall. These values are of the same order as the measured ones.

Further experimental studies in thin films and nanowires of Co, Ni, and Fe,^{8–10} as well as in a zigzag wire of Co,¹¹ confirmed the presence of the effect. But, in contrast to the previous results,^{4,5} these measurements revealed a decrease of the resistivity in the presence of a DW. The possible theoretical explanation of this phenomenon was suggested by Tatara and Fukuyama.¹² On the basis of the single-band Hubbard model with the effect of a DW included by a gauge transformation these authors calculated the second-order conductivity corrections in a weak localized regime by means of the Kubo formula. They have shown that the presence of a DW contributes to the dephasing of electrons which causes a reduction of the impurity scattering. How-

ever, as discussed by Rüdiger *et al.*,¹³ in the experiments the effect survives to much higher temperatures as predicted by this theory. The possible origin of the observed enhancement of the conductance was attributed to the AMR due to the reorientation of the flux closure caps which arise in a zero-field state near the surface of a specimen.

Ab initio studies of the magnetoresistance due to a DW in pure Fe, Co, and Ni were reported by van Hoof *et al.*¹⁴ These authors used the embedding Green-function technique based on the linearized augmented plane-wave method within the local spin-density approximation (LSDA). The ballistic conductance was calculated by means of the Landauer formula. A DW was simulated by a spin-spiral region of finite width sandwiched by two semi-infinite leads. At thicknesses of DW's adapted to experimental values the calculated amplitude of the magnetoresistance was $\sim 0.1\%$. The importance of the realistic electronic structure for the discussed phenomenon was shown by a comparison with the two-band model. Due to a proper description of quasidegenerate states at the Fermi energy in the *ab initio* approach the amplitude of the effect was much larger. In addition, the calculated thickness dependence of the magnetoresistance agrees well with the experimentally obtained $(1/\lambda_{DW})$ behavior, in contrast to $(1/\lambda_{DW})^2$ predicted by the two-band model. A huge amplitude of the effect, $\sim 60\%$, was found for the abrupt DW ($\lambda_{DW}=0$). All the calculations have shown an increase of the resistance in the presence of a DW.

Recently Kudrnovský *et al.*¹⁵ studied the effect of disorder on the DW resistance from first principles. By means of the surface Green-function technique based on the tight-binding linear muffin-tin orbital method (TB-LMTO) these authors calculated within the coherent potential approximation the electronic structure of the system of two semi-infinite leads of fcc Co sandwiching the sample of a substitutional disordered binary alloy containing a DW. Both nonmagnetic, Cu, and magnetic, Ni, Cr, impurities were considered. The conductance was calculated with the Landauer-Büttiker approach. It was shown that disorder decreases the GMR due to a DW. In general, the effect of impurities was important for very thin DW's only.

In this work we studied the magnetoresistance due to a DW in pure iron theoretically on the basis of an *ab initio* calculation of the electronic structure by means of the linear muffin-tin orbital method (LMTO) generalized for noncollinear magnets. The diffusive conductivity was calculated within the Boltzmann formalism. We consider the system consisting of the regions of collinear magnetic order, that is, ferromagnetic domains, alternated with regions of spiral magnetic order, the DW's. The dependencies of the GMR on the angle between the magnetization of neighboring domains, on the thickness of a DW, and the domain size are discussed.

II. THEORETICAL MODEL AND METHOD OF CALCULATION

We have studied pure iron in a superlattice structure with N atomic layers along (001) direction of the bcc lattice with a lattice constant $a=2.87$ Å. In order to model a Bloch wall

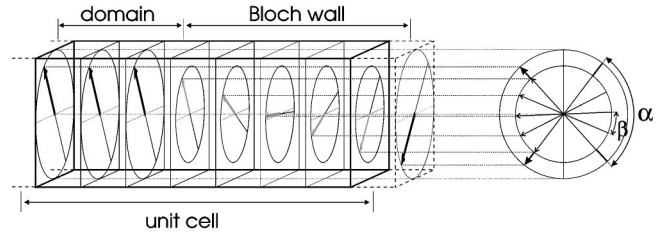


FIG. 1. The unit cell of the superlattice of pure Fe with noncollinear magnetic profile modeling the domain wall.

we have chosen the following noncollinear magnetic configuration, shown schematically in Fig. 1. All the magnetic moments are oriented perpendicular to the (001) direction. The first n monolayers (ML's) of the unit cell represent the intrinsically ferromagnetic domain. The next m atomic layers form a DW with a constant angle β between the magnetizations in the neighboring atomic layers. The total number of atoms is $N=n+m$. The angle between the magnetizations of a domain in the neighboring cells α has been varied from 180° to 0° . This way we imitated the effect of the applied external magnetic field from zero to the saturation field. The thickness of a DW was varied from 5 to 15 ML's and the domain size from 1 to 19 ML's. The described configuration can be treated as a magnetic spiral along the fourfold axis of a tetragonal lattice with N atoms per unit cell.

The calculations of the electronic structure of the superlattices were done by means of the LMTO method¹⁶ generalized for noncollinear, in particular spiral, magnets. The details of the method can be found elsewhere.¹⁷ The self-consistent band-structure calculations were carried out on a grid of 5760 \mathbf{k} points in the Brillouin zone. For the calculation of the conductivity tensor a mesh of 230496 \mathbf{k} points has been used. All the \mathbf{k} -integrated functions were computed with the tetrahedron method.¹⁸

The transport properties were calculated by means of the linearized Boltzmann equation in relaxation time approximation,

$$-e \left(\frac{\partial f_k^o}{\partial \epsilon_k(\alpha)} \right) \mathbf{v}_k(\alpha) \mathbf{E} = \frac{g_k(\alpha)}{\tau}. \quad (1)$$

$g_k(\alpha)$ is the deviation of the electron distribution function from the Fermi-Dirac equilibrium distribution f_k^o if an external electric field \mathbf{E} is applied. $\mathbf{v}_k(\alpha)$ is the velocity of the electrons. The scattering of the electrons is described by means of an isotropic relaxation time τ . e is the charge of the electron and k is a shorthand notation for wave vector \mathbf{k} and band index ν . With the current density

$$\mathbf{j}(\alpha) = 2e \sum_{\mathbf{k}} \mathbf{v}_k(\alpha) g_k(\alpha) \quad (2)$$

and Ohm's law

$$\mathbf{j}(\alpha) = \hat{\sigma}(\alpha) \mathbf{E} \quad (3)$$

the conductivity tensor becomes

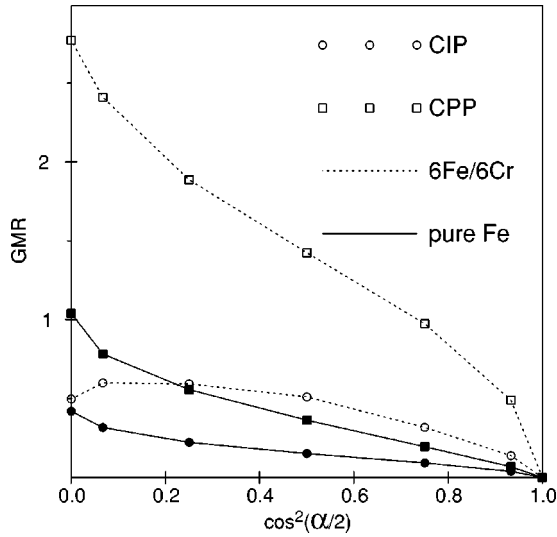


FIG. 2. Orientation dependence of the CIP- and CPP-GMR due to a DW in Fe in comparison to Fe/Cr.

$$\hat{\sigma}(\alpha) = 2e^2\tau \sum_k \delta[\epsilon_k(\alpha) - \epsilon_f] \mathbf{v}_k(\alpha) \otimes \mathbf{v}_k(\alpha). \quad (4)$$

The GMR ratio due to a DW as a function of α is

$$\text{GMR}(\alpha) = \frac{\sigma(0) - \sigma(\alpha)}{\sigma(\alpha)}. \quad (5)$$

Because of the tetragonal symmetry of the considered superlattice the conductivity tensor consists of two independent components. $\sigma_{xx} = \sigma_{yy}$ is the in-plane conductivity (CIP) and causes CIP-GMR, i.e., for the current parallel to the plane of rotation of magnetic moments in the Bloch wall, whereas σ_{zz} is the conductivity for the current perpendicular to this plane (CPP) and causes CPP-GMR.

III. RESULTS AND DISCUSSION

The calculated orientation dependence of the CIP- and the CPP-GMR in the superlattice of pure iron with both the thickness of a DW and the domain size fixed at 6 ML's is shown in Fig. 2. For the values of α at 30°–150° both the CIP- and the CPP-GMR show cos-like behavior. The variation of GMR for these angles is most likely determined by smooth changes in the exchange interaction between the magnetic moments. In the ferromagnetic ($\alpha=0$) and the antiferromagnetic ($\alpha=180^\circ$) configurations the additional symmetry affects the topology of the Fermi surface drastically. These changes give most probably rise to the deviation from the cos-like dependence for the angles 0°–30° and 150°–180°. The calculated amplitudes of the GMR due to a DW, about 40% for the CIP and 100% for the CPP geometry respectively, are much larger than the measured ones. The reported experimental values vary in the range 0.5–5%. The reason for this discrepancy is related to the very thin DW (9 Å) in the calculation. Realistic systems, films, and nanowires show DW thickness of 100–1000 Å.¹³

It is interesting to compare the discussed dependence in

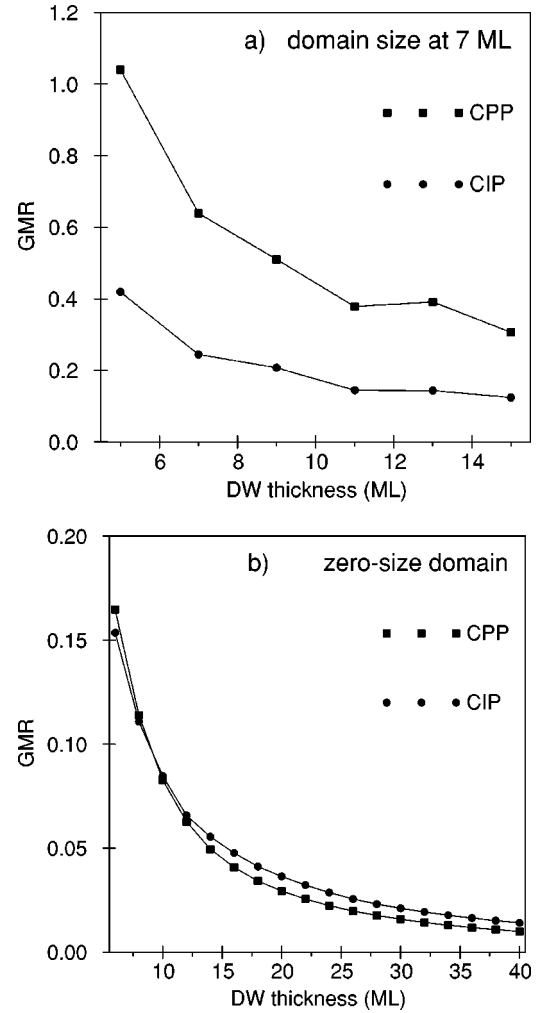


FIG. 3. Dependence of GMR on the DW thickness of the 180°-Bloch wall for (a) fixed domain size at 7 ML's and (b) zero-size domains (pure spiral).

pure Fe with the orientation dependence of GMR in 6 Fe/6 Cr superlattices calculated earlier by the authors with the same method¹⁹ (shown by the broken line in Fig. 2). This way one can distinguish the effect of the chemically different interlayer on the GMR. First, the presence of Cr increases the amplitude of the effect, about 1.4 times for the CIP- and 2.7 times for the CPP-GMR respectively. Next, in this case there are considerable deviations from the cos-like dependence for all values α . In particular, the maximum value of CIP-GMR is shifted away from the antiferromagnetic configuration.

From now on we will discuss the 180° DW. Figure 3 shows GMR as a function of the DW thickness. For the domain size fixed at 7 ML's [Fig. 3(a)] both the CIP- and the CPP-GMR decrease monotonically except a small deviation at 13 ML's. The increase of the DW thickness smoothes the potential difference due to the exchange interaction continuously and decreases the GMR effect. At the same time the periodic sequence of the alternating domains of the majority and the minority magnetization in our model gives rise to energetically localized electronic states. The crossing of the Fermi level by one of these states causes most likely the small deviation from the monotonic decrease in the consid-

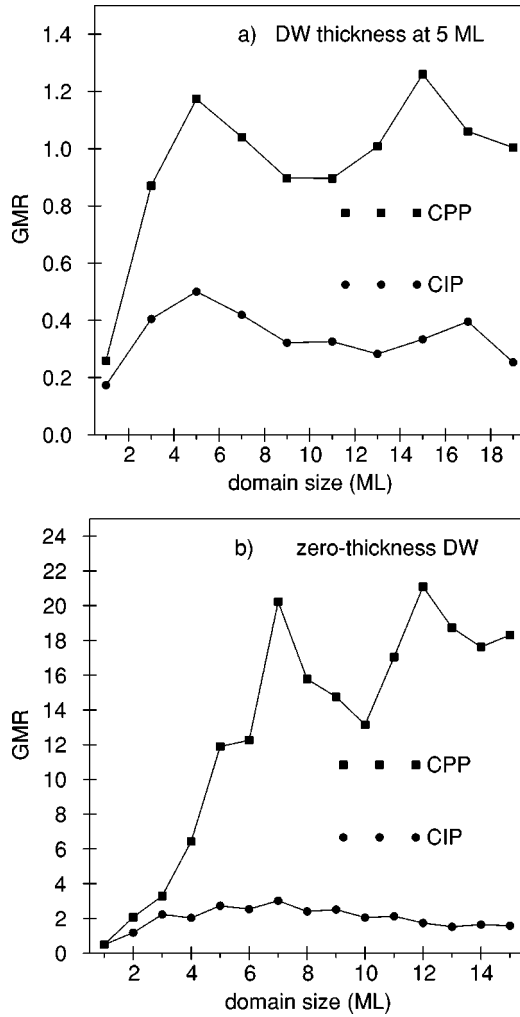


FIG. 4. Dependence of the GMR on the domain size of the 180°-Bloch wall for (a) the DW thickness fixed at 5 ML's and (b) the abrupt DW (antiferromagnetic configuration).

ered dependence. The role of these quantum well states is discussed below in detail. For zero domain size [Fig. 3(b)], i.e., a pure spiral without collinear regions, both the CIP- and the CPP-GMR decrease monotonically with the increase of the DW thickness. Namely, the function shows $(1/\lambda_{DW})$ -behavior in accordance with the results of van Hoof *et al.*¹⁴

Figure 4 shows the CIP- and the CPP-GMR as a function of domain size. For the 5-ML-thick Bloch wall [Fig. 4(a)] and varying domain size of 1–19 ML's there are two prominent peaks of the CPP-GMR. The CIP-GMR also shows oscillations but with much smaller amplitude. This oscillatory behavior is especially pronounced for zero-thickness DW's, i.e., the collinear magnet with abruptly alternating domains [Fig. 4(b)]. These oscillations are caused by quantum well states. In order to explain this point in detail we now turn to the Kronig-Penney (K-P) model.

The correspondence between the discussed superlattice and the K-P model is schematically shown in Fig. 5. The periodic sequence of rectangular barriers and wells of equal width in the z direction represents the domains of the major-

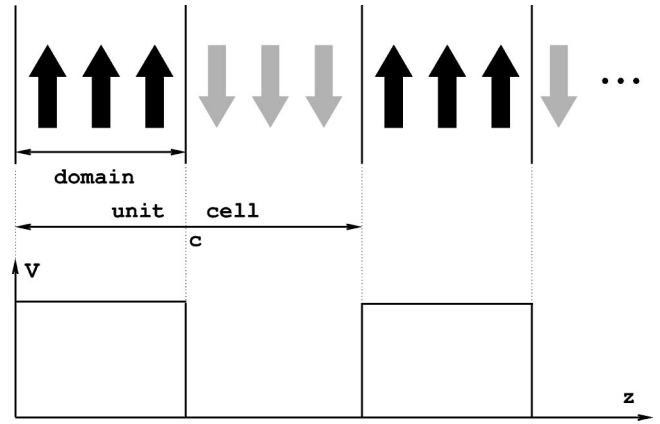


FIG. 5. Correspondence between the superlattice with the abrupt DW and the Kronig-Penney model.

ity and the minority magnetization in the superlattice. The height of a potential step V corresponds to the exchange splitting. The dispersion relation for the one-dimensional 1D K-P model is well known from the quantum mechanics text books.²⁰ In order to consider three-dimensional motion of the electrons we assume that at fixed z for any x and y the potential is the same as for $x=y=0$. The dispersion relation for this quasi-3D model,

$$E(k_{\parallel}, k_z) = E(0, k_z) + k_{\parallel}^2, \quad (6)$$

possesses the axial symmetry with respect to the k_z direction. $E(0, k_z)$ corresponds to the 1D K-P model. Next, we assume a and $c = a \cdot M$ to be the lattice constants of the tetragonal unit cell. The ratio M represents the domain size. It is convenient to introduce dimensionless parameters $\nu = V \cdot a^2$ and $\epsilon = E \cdot a^2$ instead of the potential and the energy, and $\kappa_{\parallel} = k_{\parallel} \cdot a$, $\kappa_z = k_z \cdot c$, $0 \leq \kappa_z \leq \pi$ instead of the components of the Bloch vector. Finally, we introduce the electron density n_{el} per cubic unit cell with $c = a$ as an additional parameter of the model. With the dispersion relation Eq. (6) and n_{el} it is easy to determine the position of the Fermi level and to calculate the Boltzmann conductivity according to Eq. (4).

The left-hand panel of Fig. 6 shows σ_{zz} and the CPP-GMR for the K-P model with $\nu=7$ and $n_{el}=0.5$ as a function of the domain size calculated on a grid of 500 points for M of 1–15. As a reference value for the GMR, i.e., $\sigma(0)$ in Eq. (5), the conductivity of the free-electron gas was used. Both σ and the GMR show oscillations. The minima of σ correspond, of course, to the maxima of GMR. The energy-band structure and the Fermi surface (FS) shown in Fig. 7 explain the origin of these oscillations. The three values of M , 2.56, 3.19, and 4.21, correspond to the first two maxima of $\sigma(M)$ and the minimum in between. At $M=2.56$ the Fermi level crosses the second energy band near the lower edge of the quasigap. This crossing produces an ellipsoidal sheet of the FS with a large contribution to σ_{zz} . Another sheet of the FS stems from the first band. Because of the cylindrical shape around the κ_z axis its contribution to the conductivity in z direction is negligible. For $M=3.19$ the Fermi level is located near the upper edge of the quasigap between the second and the third energy bands. The FS con-

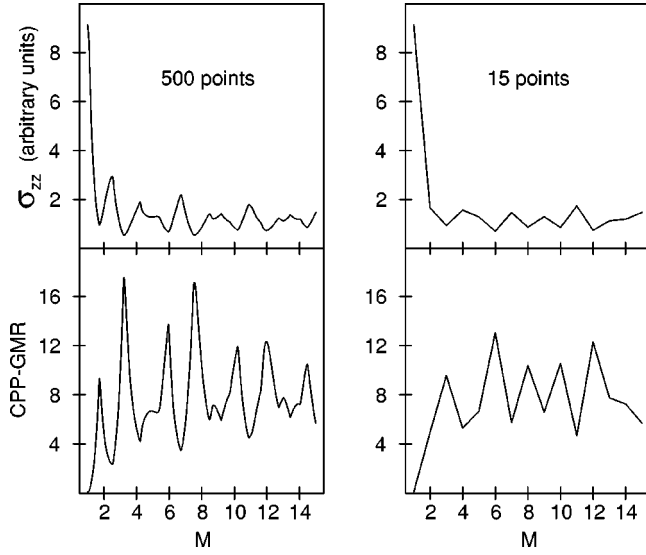


FIG. 6. Conductivity oscillations in the Kronig-Penney model with parameters $\nu=7$, $n_{el}=0.5$.

sists of two nearly cylindrical sheets with a small contribution to σ_{zz} . The crossing of the Fermi level by the third energy band at $M=4.21$ produces again a large ellipsoidal sheet giving rise to the maximum of the conductivity. In general, the increase of the domain size at a fixed exchange splitting increases the quantum well strength $V \cdot c^2$. It leads

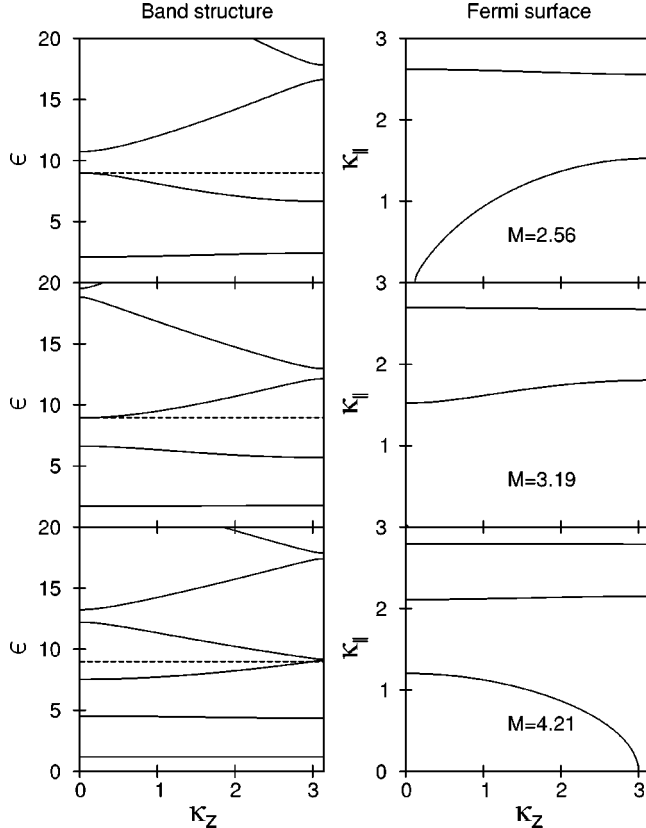


FIG. 7. Quantum well states at the Fermi level in the Kronig-Penney model.

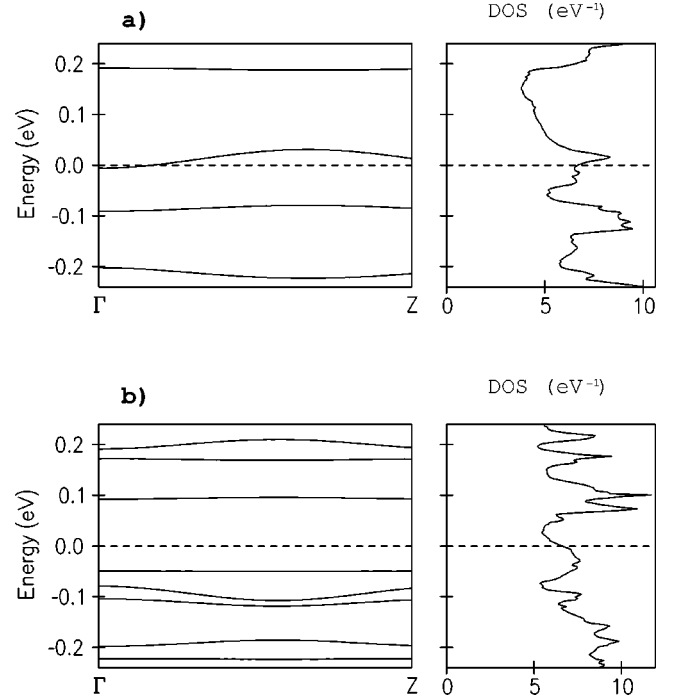


FIG. 8. Quantum well states at the Fermi level in the *ab initio* calculation for the superlattice of pure Fe with abrupt DW with fixed domain size fixed (a) at 6 and (b) at 7 ML's.

to the drop of the energy bands. The Fermi level, which value is nearly independent on M , alternatively either crosses one of the low-dispersion quantum well bands, or is located in a quasigap. The crossing produces an ellipsoidal sheet of the FS with a large contribution to the conductivity in the z direction, while with the Fermi level in a quasigap the FS consists of several nearly cylindrical sheets with negligible contribution to σ_{zz} . The same mechanism produces also the oscillation in the CIP conductivity but its amplitude is much smaller. It should be noted that the parameters of the K-P model were chosen quite arbitrarily and do not necessarily match the corresponding values in Fe. Nonetheless, the discussed oscillatory behavior is reproduced for a wide range of these parameters.

While in the K-P model the domain size can be changed continuously, the realistic crystal structure is restricted to integer numbers M . This fact complicates the direct comparison between the maxima of the conductivity and the quantum well states. In order to demonstrate the effect of aliasing to the structure the right-hand panel of Fig. 6 shows $\sigma(M)$ and $GMR(M)$ calculated for a discrete numbers M with $\Delta M=1$. Instead of seven maxima this dependence shows only five maxima and its positions are shifted. Nevertheless, the role of the quantum well states in this effect can also be confirmed with the *ab initio* calculation. Figure 8 shows the *ab initio* energy-band structure in the Γ -Z direction calculated for the superlattice of pure Fe with the abrupt DW for the domain size fixed at 6 and 7 ML's [Figs. 8(a) and (b) respectively]. For the energies at -0.25 to 0.25 eV around the Fermi level there is a set of the low-dispersion quantum well bands separated by quasigaps. The localized character of these states can be seen from the density of states, also

shown in this picture. For the domain size at 6 ML's one of the bands crosses the Fermi level, while at 7 ML's the Fermi level is located at the middle of the quasigap. At the same time the CPP-GMR [see Fig. 4(b)] increases strongly between these two values. Moreover, there is a feature on this dependence at 6 ML's, which is most likely connected with an unresolved minimum.

IV. CONCLUSIONS

We have studied GMR caused by a Bloch wall in pure Fe on the basis of *ab initio* calculations of the electronic structure in a superlattice geometry. The calculated orientation dependence of the GMR ratio was shown to be cos-like excluding the angles in the vicinity of both ferromagnetic and antiferromagnetic magnetic ordering. Comparing the present calculations with our previous results for Fe/Cr superlattices we have shown that due to the chemically different interlayer there are considerable deviations from the cos-like behavior and the amplitude of the effect for both CIP- and CPP-GMR

is larger than for pure Fe. It was shown that the oscillations of GMR as a function of a domain size stem from the quantum well states crossing the Fermi level.

As we already mentioned, a very thin DW modeled in our calculation results in a much larger GMR effect as compared to the measured values in thin films and nanowires. Recently Bruno²¹ discussed the possibility of a very narrow domain wall caused by a constriction which size does not exceed the characteristic size of the constriction. In the case of an atomic point contact this length is several nanometers. García *et al.* studied ballistic magnetoresistance point contacts of Ni, Co,²² and Fe,²³ and measured in fact a very large amplitude of the GMR ratio, 200–300% for Ni and Co and ~30% for Fe, respectively. Although the origin of these large MR ratios is not yet clear the results of this paper show that an abrupt DW can give large GMR values in agreement with the results of Refs. 14 and 15. A direct comparison, however, is impossible since the shape of the sample is not included in the calculation.

*Corresponding author. Email address: yavorsky@physik.uni-halle.de

¹M.N. Baibich, J.M. Broto, A. Fert, F. Nguyen Van Dau, F. Petroff, P. Etienne, G. Creuzet, A. Friederich, and J. Chazelas, *Phys. Rev. Lett.* **61**, 2472 (1988); G. Binasch, P. Grünberg, F. Saurenbach, and W. Zinn, *Phys. Rev. B* **39**, 4828 (1989).

²See G.R. Taylor, A. Isin, and R.V. Coleman, *Phys. Rev.* **165**, 621 (1962), and references therein.

³G.G. Cabrera and L.M. Falicov, *Phys. Status Solidi B* **61**, 539 (1974).

⁴M. Viret, D. Vignoles, D. Cole, J.M.D. Coey, W. Allen, D.S. Daniel, and J.F. Gregg, *Phys. Rev. B* **53**, 8464 (1996).

⁵J.F. Gregg, W. Allen, K. Ounadjela, M. Viret, M. Hehn, S.M. Thompson, and J.M.D. Coey, *Phys. Rev. Lett.* **77**, 1580 (1996).

⁶P.M. Levy and S. Zhang, *Phys. Rev. Lett.* **79**, 5110 (1997).

⁷K. Wang, S. Zhang, and P.M. Levy, *Phys. Rev. B* **54**, 11 965 (1996).

⁸K. Hong and N. Giordano, *J. Phys.: Condens. Matter* **10**, L401 (1998).

⁹Y. Otani, S.G. Kim, K. Fukamichi, O. Kitakami, and Y. Shimada, *IEEE Trans. Magn.* **34**, 1096 (1998); Y. Otani, K. Fukamichi, O. Kitakami, Y. Shimada, B. Pannetier, J.P. Noziers, T. Matsuda, and A. Tonomura, in *Magnetic Ultrathin Films Multilayers and Surfaces*, edited by J. Tobin, D. Chambliss, D. Kubinski, K. Barmak, P. Dederichs, W. de Jonge, T. Katayama, and A. Schuhl, MRS Symposia Proceedings No. 475 (Materials Research Society, San Francisco, 1997); S.G. Kim, Y. Otani, K. Fukamichi, S. Yuasa, M. Nyvlt, and T. Katayama, *J. Magn. Magn. Mater.*

198-199, 200 (1999).

¹⁰U. Rüdiger, J. Yu, S. Zhang, A.D. Kent, and S.S.P. Parkin, *Phys. Rev. Lett.* **80**, 5639 (1998).

¹¹T. Taniyama, I. Nakatani, T. Namikawa, and Y. Yamazaki, *Phys. Rev. Lett.* **82**, 2780 (1999); T. Taniyama, I. Nakatani, T. Yakabe, and Y. Yamazaki, *Appl. Phys. Lett.* **76**, 613 (2000).

¹²G. Tataru and H. Fukuyama, *Phys. Rev. Lett.* **78**, 3773 (1997).

¹³U. Rüdiger, J. Yu, L. Thomas, S.S.P. Parkin, and A.D. Kent, *Phys. Rev. B* **59**, 11 914 (1998); U. Rüdiger, J. Yu, S.S.P. Parkin, and A.D. Kent, *J. Magn. Magn. Mater.* **198-199**, 261 (1999).

¹⁴J.B.A.N. van Hoof, K.M. Schep, A. Brataas, G.E.W. Bauer, and P.J. Kelly, *Phys. Rev. B* **59**, 138 (1998).

¹⁵J. Kudrnovský, V. Drchal, I. Turek, P. Středa, and P. Bruno, *Surf. Sci.* **482-485**, 1107 (2001).

¹⁶O.K. Andersen, *Phys. Rev. B* **12**, 3060 (1975).

¹⁷L.M. Sandratskii, *Adv. Phys.* **47**, 91 (1998).

¹⁸P.E. Blöchl, O. Jepsen, and O.K. Andersen, *Phys. Rev. B* **49**, 16 223 (1994).

¹⁹B.Yu. Yavorsky, I. Mertig, A.Ya. Perlov, A.N. Yaresko, and V.N. Antonov, *Phys. Rev. B* **62**, 9586 (2000).

²⁰E. Merzbacher, *Quantum Mechanics* (John Wiley & Sons, New York, 1970), p. 621.

²¹P. Bruno, *Phys. Rev. Lett.* **83**, 2425 (1999).

²²N. García, M. Muñoz, and Y.-W. Zhao, *Phys. Rev. Lett.* **82**, 2923 (1999); G. Tataru, Y.-W. Zhao, M. Muñoz, and N. García, *ibid.* **83**, 2030 (1999).

²³N. García, M. Muñoz, and Y.-W. Zhao, *Appl. Phys. Lett.* **76**, 2586 (2000).